Synthesis and Characterization of Ta_2O_5−ZrO_2 Systems: Structure, Surface Acidity, and Catalytic Properties.

Bárbara Samaranch,[†] Pilar Ramírez de la Piscina,*[,†] Guillaume Clet,[‡] Marwan Houalla,[‡]
Patrick Gélin,[§] and Narcís Homs*[,†]

Departament de Química Inorgànica and Institut de Nanociència i Nanotecnologia, Universitat de Barcelona, C/ Martí i Franquès 1-11, 08028 Barcelona, Spain, Laboratoire de Catalyse et Spectrochimie (UMR CNRS 6506), ENSICAEN−Université de Caen, 6 Boulevard du Maréchal Juin, 14050 Caen Cedex, France, and Laboratoire d'Application de la Chimie à l'Environnement (UMR CNRS 5634), Université Claude Bernard Lyon 1, 43 Boulevard du 11 Novembre 1918, Bâtiment Chevreul, 69622 Villeurbanne Cedex, France

Received November 13, 2006. Revised Manuscript Received January 15, 2007

The preparation of binary materials based on Ta_2O_5−ZrO_2 by a sol−gel method and with a wide range of compositions is reported (Ta_2O_5 nominal content from 4 to 74% w/w). Materials were characterized by X-ray diffraction, and infrared and Raman spectroscopy. Their acidic characteristics were evaluated from the model reaction of 2-propanol dehydration and the adsorption of CO at 77 K and 2,6-dimethylpyridine at 373 K, both followed by infrared spectroscopy. Increasing tantalum content brings about a development of a surface TaO_x phase followed by a progressive formation of aggregates of amorphous Ta_2O_5. Increased stabilization of tetragonal zirconia was also observed with increasing Ta loading. The surface area, number and strength of Brönsted acid sites, and the catalytic activity in the 2-propanol dehydration increase with the increase in tantalum content up to ca. 50% w/w Ta_2O_5. A surface area of 103 $m^2\ g^{-1}$ was obtained for a solid with a Ta_2O_5 content of 53% w/w after calcination at 873 K. The abundance of Brönsted acid sites, determined by lutidine adsorption, and their strength, determined by CO adsorption at 77 K, correlated with the catalytic activity in the 2-propanol dehydration.

Introduction

Much work has been devoted to the preparation of ZrO_2-based binary oxides to be used as catalysts or as supports in catalyst preparation.[1−6] A subject of particular interest is the characterization of surface species that determine the acidity of solids and consequently can condition their catalytic properties.[7−9] This aspect is related to the interest of developing robust and stable solid acids with strong Brönsted acid sites to be used as catalysts and replace acids operating in solution.[10,11] Stabilization of small tetragonal ZrO_2 particles is also of interest because it appears to be associated with an observed increase in the surface area of binary systems.[8,12] Most of the binary systems studied, to date, involve metals of groups 4, 5, and 6 of the Periodic Table, but not much attention has been paid to tantalum. However, hydrated tantalum oxide has shown high catalytic activities in acid-catalyzed reactions such as the esterification of methacrylic acid with methanol, the alkylation of benzene with ethane, or the isomerization of 1-butene.[13] In the absence of water, hydrated tantalum oxide has mainly shown Lewis acidity, but Brönsted sites were generated by steam treatment.[13] The study of the binary SiO_2−Ta_2O_5 system has shown that acid sites were generated when the binary system was compared with pure tantalum oxide.[14,15] This background led us to study the ZrO_2−Ta_2O_5 system. Because the preparation method conditions the textural and surface properties of mixed oxides and therefore their catalytic behavior, we have adopted sol−gel synthesis routes. Such procedures were shown to be very appropriate for the synthesis of high-surface-area binary oxide systems with adequate surface properties.[6] In the present study, we report the preparation of ZrO_2-supported tantalum samples by a sol−gel method. Solids with a wide composition range were prepared and characterized by several techniques. The abundance of acid sites was quantitatively evaluated by 2,6,-dimethylpyridine (lutidine) adsorption followed by FTIR, and their acidic strength was evaluated by CO adsorption at 77 K. The results correlate

---

* Corresponding author. Tel: 34-934037056. Fax: 34-934907725. E-mail: narcis.homs@qi.ub.es (N.H.); pilar.piscina@qi.ub.es (P.R.d.l.P.).
[†] Universitat de Barcelona.
[‡] ENSICAEN-Université de Caen.
[§] Université Claude Bernard Lyon 1.

(1) Hino, K.; Arata, K. *J. Chem. Soc., Chem. Commun.* **1987**, 1259.
(2) Arata, K. *Appl. Catal.* **1996**, *146*, 3.
(3) Pieck, C. L.; Bañares, M. A.; Vicente, M. A.; Fierro, J. L. G. *Chem. Mater.* **2001**, *13*, 1174.
(4) Su, S. C.; Bell, A. T. *J. Phys. Chem. B* **1998**, *102*, 7000.
(5) Vu, T. N.; van Gestel, J.; Gilson, J. P.; Collet, C.; Dath, J. P.; Duchet, J. C. *J. Catal.* **2005**, *231*, 453.
(6) Samaranch, B.; Ramírez de la Piscina, P.; Clet, G.; Houalla, M.; Homs, N. *Chem. Mater.* **2006**, *18*, 1581.
(7) Santiesteban, J. G.; Vartuli, J. C.; Han, S.; Bastian, R. D.; Chang, C. D. *J. Catal.* **1997**, *168*, 431.
(8) Scheithauer, M.; Grasselli, R. K.; Knözinger, H. *Langmuir* **1998**, *14*, 3019.
(9) Onfroy, T.; Clet, G.; Houalla, M. *J. Phys. Chem. B* **2005**, *109*, 3345.
(10) Clark, J. H. *Acc. Chem. Res.* **2002**, *35*, 791.
(11) Okuhara, T. *Chem. Rev.* **2002**, *102*, 3641.
(12) Valigi, M.; Gazzoli, D.; Pettiti, I.; Mattei, G.; Colonna, S.; De, Rossi, S.; Ferraris, G. *Appl. Catal., A* **2002**, *231*, 159.
(13) Ushikubo, T.; Wada, K. *Appl. Catal.* **1990**, *67*, 25.
(14) Guiu, G.; Grange, P. *J. Catal.* **1995**, *156*, 132.
(15) Guiu, G.; Grange, P. *Bull. Chem. Soc. Jpn.* **1994**, *67*, 2716.

10.1021/cm062704z CCC: $37.00

with the performance of catalysts in the dehydration of 2-propanol.

Experimental Section

Propanol solutions of tantalum ethoxide and zirconium propoxide were prepared under an inert atmosphere and mixed over an aqueous solution of propanol. Both solutions were added at room temperature by independent addition pumps, with vigorous external mechanical stirring. The suspension was maintained at 343 K for 6 h with stirring and then at 298 K for 16 h. After filtration, the solids were dried at 383 K and subsequently calcined in air at 873 K for 4 h. The samples were labeled *x*TaZr, where *x* is the nominal percent w/w Ta_2O_5 in the solid.

The chemical composition of the samples was determined using inductively coupled plasma with atomic emission spectroscopy (ICP-AES) in an Optima Perkin-Elmer 3200RL apparatus.

Nitrogen adsorption at 77 K was used to determine the BET surface area by means of a Micromeritics ASAP9000 instrument.

X-ray diffraction (XRD) profiles were collected in a Siemens D-500 powder X-ray diffractometer equipped with a graphite monochromator and a Cu target. Diffractograms were recorded at a step width of 0.02° and by counting 10 s at each step.

Raman spectroscopy was performed with a Jobin Yvon T64000 instrument using an Ar ion laser as an illumination source (514.5 nm) and a CCD detector cooled to 140 K. The collection optics system was used in the backscattering configuration, and the apparatus was operated in Macro Raman mode with a resolution better than 2 cm^{-1}. The laser power was 70 mW. Samples were studied in the 20−1200 cm^{-1} range.

Fourier transform infrared experiments (FTIR) of lutidine adsorption and CO adsorption at 77 K were carried out on a Nicolet Magna IR550, equipped with a DTGS detector. Infrared spectra were obtained at a resolution of 4 cm^{-1} by collecting 128 scans. Samples were pressed into pellets (∼ 20 mg; 2 cm^2).

For lutidine adsorption, samples were first treated under a vacuum at 723 K for 1 h, then in O_2 ($P_{O_2} = 13.3$ kPa) for 1 h and finally evacuated for 1 h at 473 K. Lutidine adsorption was carried out at 373 K ($P = 133$ Pa) followed by thermal desorption from 373 to 523 K under a vacuum. Spectra were recorded at room temperature. The number of Brönsted and Lewis acid sites titrated by lutidine was calculated using integrated molar absorption coefficient values of $\epsilon = 6.8$ cm μmol^{-1} (for the sum of the ($\nu_{8a} + \nu_{8b}$) vibrations of protonated lutidine at ca. 1640 and 1628 cm^{-1}) and 4.35 cm μmol^{-1} (for the sum of the ($\nu_{8a} + \nu_{8b}$) vibrations of coordinated lutidine), respectively.[16]

For CO adsorption at 77 K, self-supported wafers of samples were introduced into a homemade IR cell, allowing in situ high-temperature treatments and low-temperature measurements.[17] Samples were treated in an oxygen flow at 723 K for 15 min (heating rate of 5 K min^{-1}) and outgassed in a vacuum for 1 h at 723 K before cooling to liquid nitrogen temperature. Ten Torr CO was then admitted, the CO pressure was progressively decreased, and the spectra were recorded. The same procedure was performed upon re-admitting CO on the sample, and the phenomenon was fully reversible.

Catalytic reaction of 2-propanol dehydration was measured in a continuous flow glass microreactor at atmospheric pressure and 453 K. Prior to the catalytic test, samples were treated under Ar at 723 K and then cooled to the reaction temperature. The reactant mixture was a feed of argon saturated with 2-propanol vapor, generated by bubbling Ar (90 mL min^{-1}) through a saturator maintained at 273 K ($P_{2-propanol} = 1.2$ kPa). Samples (80−350 mg) diluted with inactive SiC were used for each catalytic test, giving a catalyst bed volume of 1 mL. The products were analyzed on-line with a gas chromatograph (VarianStar 3400CX) equipped with a TRACER TRB-1 column and a flame ionization detector.

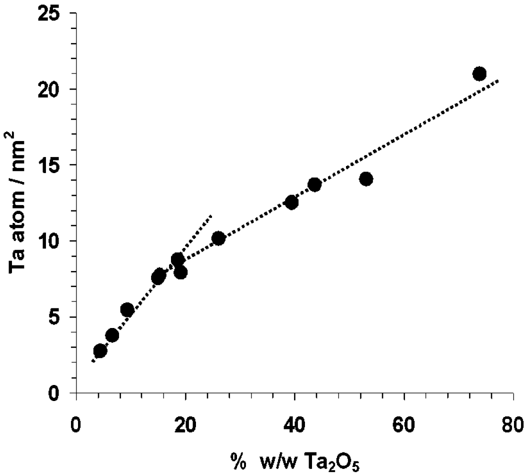

Figure 1. Tantalum surface density as a function of tantalum content.

Table 1. Characteristics of the $Ta_2O_5-ZrO_2$ Solids Calcined at 873 K and BET Surface Area and Volume Fraction of Monoclinic ZrO_2 Phases Determined by XRD[18]

sample	Ta_2O_5 (w/w)	BET SA (m^2 g^{-1})	V_m[a]
0MoZr	0	26	62
4TaZr	4.43	44	53
7TaZr	6.62	48	39
9TaZr	9.30	47	34
15TaZr	14.97	54	22
18TaZr	18.62	58	29
19TaZr	19.15	66	21
26TaZr	26.06	70	35
39TaZr	39.48	86	30
44TaZr	43.68	87	12
53TaZr	53.08	103	
74TaZr	73.85	96	
100TaZr	100	11	

[a] Volume fraction of monoclinic ZrO_2 calculated from ref 18, $V_m = 1.311X_m/(1 + 0.311X_m)$; $X_m = I(-111)_m + I(111)_m/I(-111)_m + I(111)_m + I(101)_t$.

Results and Discussion

BET Surface-Areas Measurements

Table 1 shows the composition of the catalysts prepared and the corresponding BET surface areas. Ta addition led to an increase in the surface area up to at least 53% w/w Ta_2O_5. Figure 1 shows the variation in the apparent tantalum surface density as a function of catalyst composition. A linear increase in the tantalum surface density with the Ta_2O_5 content was determined up to ca. 20% w/w Ta_2O_5, and values around 7−8 Ta atoms per nm^2 were reached for catalysts with 15−20% w/w Ta_2O_5. For higher Ta_2O_5 contents, a new linear relation was then obtained, with a lower slope. The intersection of the two straight lines fits well with the monolayer value, which had previously been determined by XPS for Ta_2O_5/ZrO_2 samples prepared by incipient wetness impregnation and in which a value of 6.3 Ta atoms/nm^2 for 7.9% w/w Ta_2O_5 had been found.[19] The sol−gel method proposed in this work for the preparation of samples led to

---

(16) Onfroy, T.; Clet, G.; Houalla, M. *Microporous Mesoporous Mater.* **2005**, *82*, 99.

(17) Echoufi, N.; Gélin, P. *J. Chem. Soc., Faraday Trans.* **1992**, *88*, 1067.

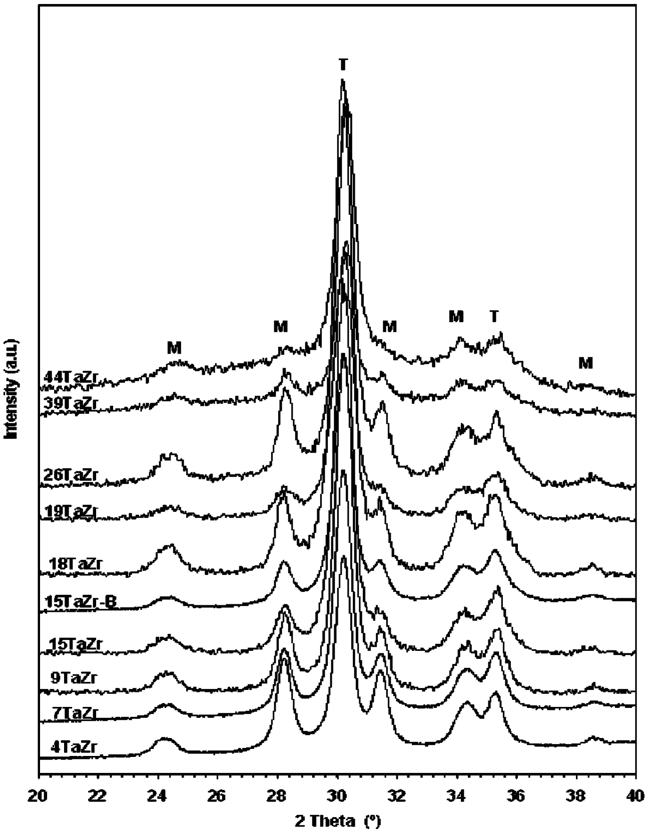

Figure 2. XRD patterns of Ta_2O_5−ZrO_2 samples (4−44% w/w Ta_2O_5) after calcination at 873 K. (T) Characteristic diffraction peaks of tetragonal ZrO_2; (M) characteristic diffraction peaks of monoclinic ZrO_2.

materials that reached the monolayer at higher tantalum contents and consequently showed higher surface-area values.

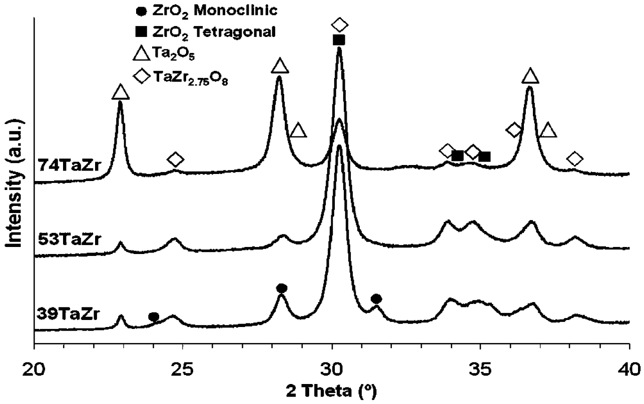

Figure 3. XRD patterns of several Ta_2O_5−ZrO_2 samples after calcination at 1073 K.

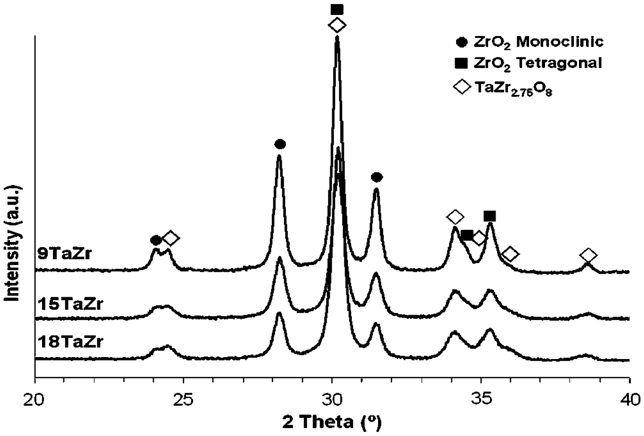

Figure 4. XRD patterns of several Ta_2O_5−ZrO_2 samples after calcination at 1223 K.

Structure of Catalysts. Figure 2 depicts the XRD patterns of the samples (calcined at 873 K) with increasing tantalum content up to 44TaZr. Only diffraction peaks corresponding to monoclinic and tetragonal ZrO_2 can be distinguished. Table 1 also shows the volume fraction of monoclinic ZrO_2 calculated from the intensity of diffraction lines corresponding to the (−111) and (111) planes of the monoclinic phase ($2\theta = 28.2$ and 31.5°, respectively) and (101) of the tetragonal phase ($2\theta = 30.2°$).[18] The addition of tantalum brings about the gradual stabilization of the tetragonal ZrO_2. Monoclinic ZrO_2 was, however, detected up to 44TaZr. XRD patterns of 53TaZr, 74TaZr, and pure Ta_2O_5 (not shown) were of poor quality, probably because of the presence of large amounts of amorphous Ta_2O_5. However, in the patterns corresponding to 53TaZr and 74TaZr, the characteristic peaks of tetragonal ZrO_2 can be distinguished. In accordance with the crystallization temperature of Ta_2O_5,[13] crystalline Ta_2O_5 was formed when pure Ta_2O_5 was calcined at 1023 K, and the sample showed an XRD pattern characteristic of orthorhombic Ta_2O_5 (ICDD 71-0639). On the other hand, no crystalline Ta_2O_5 was detected by XRD after calcination of 74TaZr, 53TaZr, or 39TaZr at 1023 K, and only when these samples were treated at a higher temperature (1073 K), were well-defined peaks corresponding to orthorhombic Ta_2O_5 observed. Note in Figure 3 that the more intense peaks of orthorhombic Ta_2O_5 are at 2θ 22.8° (001), 28.3° (1 11 0), and 36.7° (1 11 1)). From XRD patterns shown in Figure 3, the presence of mixed oxides cannot be ruled out. Specifically, peaks at $2\theta = 24.5$, 33.9, and 38.3° may correspond to the (001), and (020), (120) reflections of the solid solution $TaZr_{2.75}O_8$ (ICDD 42-0060), whose most intense peak appears at $2\theta = 30.2°$ and may overlap with the (101) reflection of tetragonal ZrO_2. Note that all the samples whose XRD patterns are depicted in Figure 3 are located on the straight line with a lower slope in Figure 1. This result is consistent with the previous findings that the crystallization temperature of Ta_2O_5 in Ta_2O_5−SiO_2 systems increases by 150 K with respect to that of pure Ta_2O_5. This difference has been attributed to an intimate mixture of the precursors of the binary system achieved in the preparation of the solids.[15]

Samples with Ta_2O_5 content lower than 20% w/w (the samples located on the straight line with the highest slope in Figure 1) did not show XRD peaks corresponding to crystalline Ta_2O_5, even following calcination at 1223 K (see Figure 4). The different behavior with respect to the crystallization of Ta_2O_5 of the samples located in the first or second part of the graph in Figure 1 must be related to the nature of the tantalum species involved, in particular, their presence as a surface phase, their nuclearity, and their interaction with the ZrO_2 support.

---

(18) Toraya, H.; Yoshimura, M.; Somiya, S. *J. Am. Ceram. Soc.* **1984**, *67*, C119.

(19) Chen, Y.; Fierro, J. L. G.; Tanaka, T.; Wachs, I. E. *J. Phys. Chem. B* **2003**, *107*, 5243.

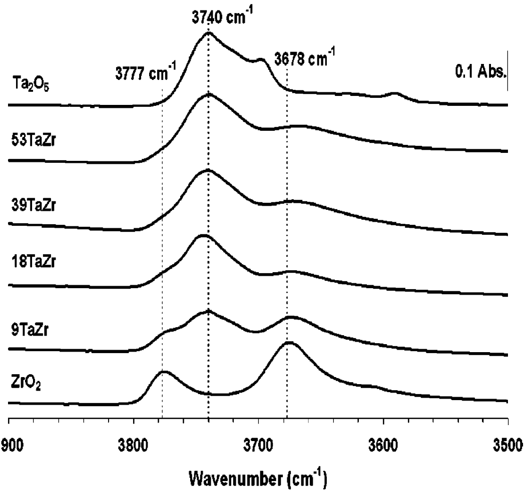

Figure 5. FTIR spectra in the υ(OH) region of Ta_2O_5−ZrO_2 samples.

IR spectroscopy can give valuable information about the nature of OH groups on the surface of the oxides we prepared. Figure 5 depicts the spectra of several TaZr samples in the υ(OH) zone. The infrared spectrum of pure Ta_2O_5 shows the main band with maximum at ca. 3740 cm^{-1}, a shoulder at 3698 cm^{-1} and a less intense band at 3591 cm^{-1}. Bands at 3777 and 3678 cm^{-1} in the spectrum of pure ZrO_2 are attributed to terminal and bridged hydroxyl groups, respectively.[20,21] The intensity of these two bands decreases with increasing Ta content in the samples and a new band, which can be assigned to the OH bonded to the tantalum species, progressively develops at 3740−3746 cm^{-1}.[22] That band could be associated with the progressive covering of the surface of ZrO_2 by tantalum species.

It has been reported that the stretching vibration mode of strong Ta═O bonds in an amorphous tantalum oxide overlayer gives a band at 2335 cm^{-1}.[23] Figure 6 shows this spectral region after subtraction of the contribution from ZrO_2. Analysis of the spectra indicates the presence of such a band for solids with a Ta_2O_5 content $\geq$39% w/w. These materials are located in the second part of the graph in Figure 1 and showed crystalline Ta_2O_5 after calcination at 1073 K.

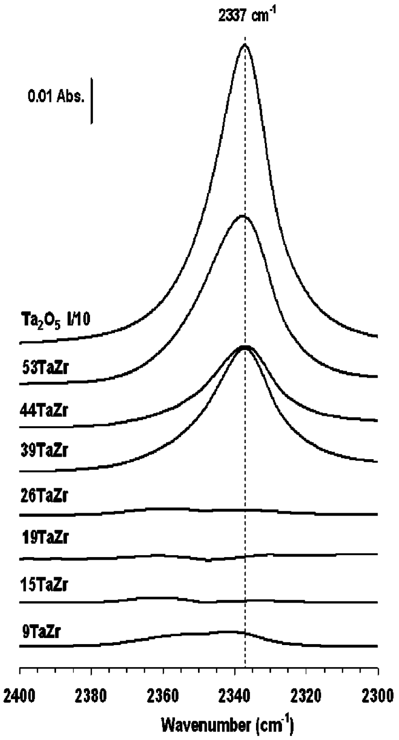

Figure 6. FTIR spectra of several Ta_2O_5−ZrO_2 samples. Spectra were obtained after substraction of the ZrO_2 spectrum.

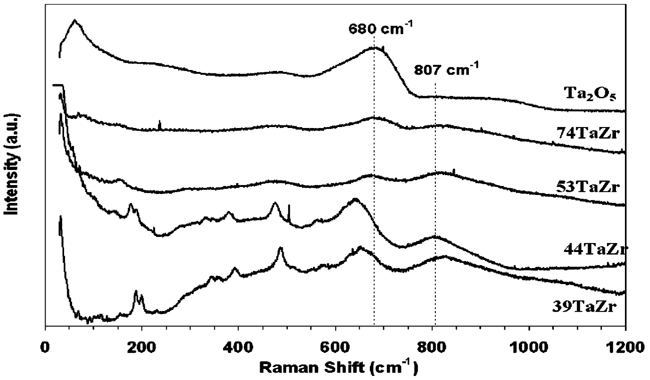

Figure 7. Raman spectra under ambient conditions of Ta_2O_5−ZrO_2 samples (39−100% w/w Ta_2O_5).

Additional structural information concerning the eventual presence of surface Ta metal oxide species can be obtained from Raman spectroscopy.[24] Figure 7 depicts the spectrum under ambient conditions of Ta_2O_5 and Ta-rich samples. The spectrum for pure Ta_2O_5 shows the main band centered at 680 cm^{-1}. A broad band at 660 cm^{-1} has been attributed to Ta−O vibration of tantalum oxyhydrate.[19] This band is clearly visible in the spectra of samples 53TaZr and 74TaZr. The 44TaZr and 39TaZr solids showed in this zone a broad and asymmetric band centered at lower Raman shift, suggesting the eventual presence of both tetragonal ZrO_2 (characteristic band at 640 cm^{-1}) and aggregates of tantalum oxyhydrate (characteristic band at 680 cm^{-1}). In addition to this band, the spectra of solids depicted in Figure 7 exhibit a band centered at 805−810 cm^{-1} that can be assigned to $\upsilon_{antisym}$(Ta−O−Ta) species in a polymeric octahedral coordination.[19] The broad and asymmetric profile observed for this band may indicate of the contribution of bands due to terminal Ta═O bonds in the above-mentioned surface species. Bands at 940−980 cm^{-1} have been related to the presence of terminal Ta═O bonds in ZrO_2- and TiO_2-supported tantalum oxide catalysts prepared by impregnation.[19] Figure 8 shows the Raman spectra of samples with lower tantalum contents. Note the absence of the band characteristic of tantalum oxyhydrate at ca. 680 cm^{-1} and the low intensity of the band centered ca. 805−810 cm^{-1} and attributed to polymeric Ta surface species. The bands appearing in the 100−650 cm^{-1} region, whose intensity decreases with tantalum content, are characteristic of monoclinic and tetragonal ZrO_2. The Raman spectrum of tetragonal ZrO_2 consists of six bands centered at 145, 268, 314, 463,

---

(20) Cerrato, G.; Bordiga, S.; Barbera, S.; Morterra, C. *Surf. Sci.* **1997**, *377*, 50.

(21) Morterra, C.; Cerrato, G.; Di Ciero, S. *Appl. Surf. Sci.* **1998**, *126*, 107.

(22) Huuhtanen, J.; Sanati, M.; Anderson, A.; Andersson, S. L. *Appl. Catal., A* **1993**, *97*, 197.

(23) Ono, H.; Koyanagi, K. *Appl. Phys. Lett.* **2000**, *77*, 1431.

(24) Baltes, M.; Kytökivi, A.; Weckhuysen, B.; Schoonheydt, R. A.; Voort, P. V. D.; Vansant, E. F.; *J. Phys. Chem. B* **2001**, *105*, 6211.

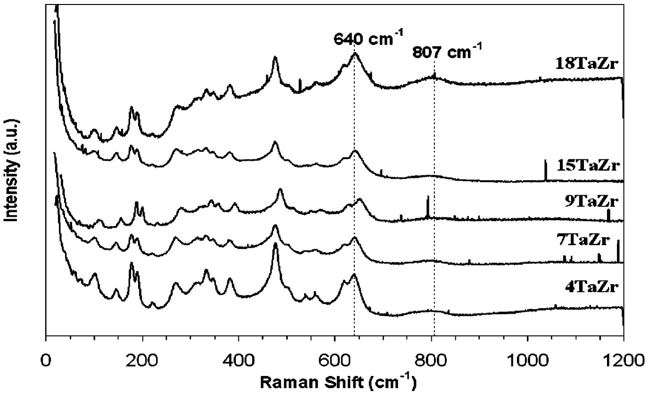

Figure 8. Raman spectra under ambient conditions of $Ta_2O_5-ZrO_2$ samples (4−18% w/w Ta_2O_5).

604 (shoulder), and 639 cm^{-1}.[25] Monoclinic ZrO_2 gives rise to a more complex spectrum that exhibits 18 Raman-active bands.[25,26] Up to a content of Ta_2O_5 of 44% w/w, the Raman spectrum of the catalysts clearly shows bands characteristic of both monoclinic and tetragonal ZrO_2 (see Figures 7 and 8). The relative intensities of the bands associated with tetragonal and monoclinic ZrO_2 make it possible to indicate a stabilization of tetragonal ZrO_2 when the Ta content increases. This agrees with the XRD experiments described above.

Development of the Acidity with Ta content: Brönsted Acid Strength. As noted before, the acidity of the materials was monitored by FTIR analysis of the adsorption of lutidine and CO. Lutidine is a specific probe molecule that is appropriate to detect and quantify both Lewis and Brönsted surface acid sites.[16,27,28] From the location of the υ_{8a} and υ_{8b} bands of the aromatic ring, it is possible to identify the nature of surface acidic centers. Quantifications of these acid sites can be achieved from the integrated molar absorption coefficients for the protonation and coordination of lutidine, which have been recently reported for lutidine adsorbed onto zirconia and zirconia-supported metal oxides.[16]

When lutidine was adsorbed on TaZr samples, two characteristic doublets arose; one of them centered at 1645 and 1628 cm^{-1} and attributed to lutidinium species formed by the interaction of lutidine with the Brönsted sites, and the other centered at 1615 and 1580 cm^{-1} and due to the interaction of lutidine with Lewis sites.[27] Figure 9 shows, as an example, spectra generated after successive lutidine adsorptions (Figure 9A) over the 19TaZr sample and subsequent desorptions at increasing temperatures (Figure 9B). Figure 10 summarizes the spectra obtained for several samples after desorption at 423 K. The spectrum of adsorbed lutidine onto ZrO_2 (Figure 10) shows two bands at 1612 and 1581 cm^{-1}. These bands are characteristic of lutidine coordinated to Lewis acid centers, and no Brönsted acid centers on ZrO_2 are detected. On the other hand, the adsorption of lutidine over Ta_2O_5 indicated the presence of surface Brönsted acid sites (see bands at 1649 and 1628 cm^{-1} in Figure 10). Moreover, a small band at 1615 cm^{-1} after lutidine adsorption indicates the simultaneous presence of Lewis acid sites. From the spectra and the integrated molar absorption coefficients for protonated and coordinated lutidine,[16] the density of Brönsted sites (μmol/g and μmol/m^2) were calculated. The results following desorption at 523 K are shown in Figures 11 and 12. The density of Brönsted acid sites (referred to by gram or square meter) increases with the tantalum content at least up to the sample 44TaZr (14 Ta atom/nm^2; Figures 11 and 12).

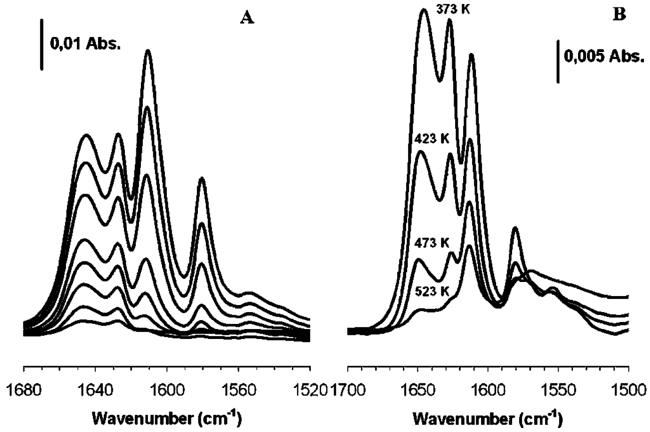

Figure 9. FTIR spectra of 19TaZr. (A) After adsorption of successive doses of lutidine at 373 K; (B) after subsequent desorption at increasing temperatures.

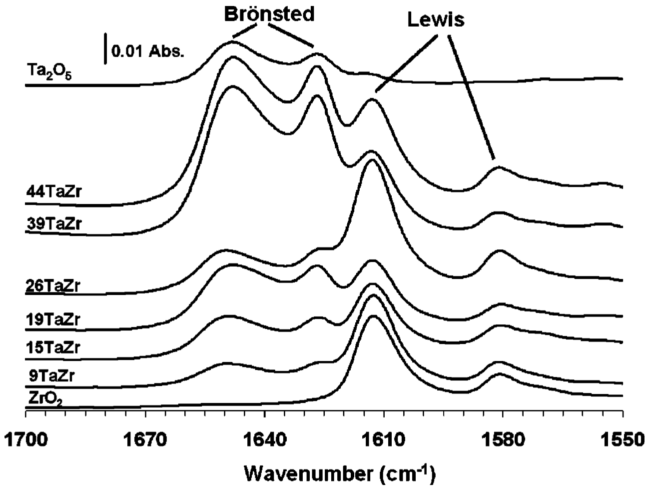

Figure 10. FTIR spectra of $Ta_2O_5-ZrO_2$ samples after lutidine adsorption at 373 K and ulterior desorption at 423 K.

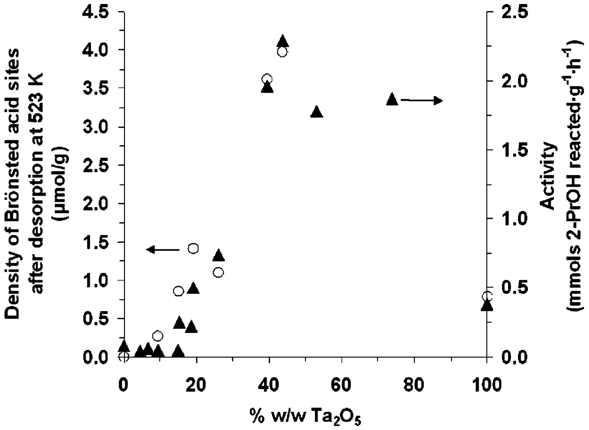

Figure 11. Density of Brönsted acid sites, determined from lutidine adsorption, and activity in the 2-propanol dehydration vs Ta_2O_5 content on $Ta_2O_5-ZrO_2$ samples.

---

(25) Fernández-López, E.; Sanchez Escribano, V.; Paniza, M.; Carnasciali, M. M.; Busca, G. *J. Mater. Chem.* **2001**, *11*, 1891.

(26) Valmalette, J. Ch.; Isa, M. *Chem. Mater.* **2002**, *14*, 5098.

(27) Jacobs, P. A.; Heylen, C. F. *J. Catal.* **1974**, *34*, 267.

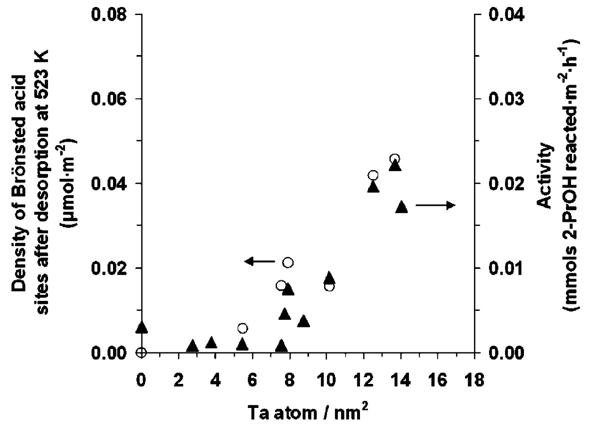

Figure 12. Density of Brönsted acid sites and activity in the 2-propanol dehydration referred by unit surface area vs tantalum surface density on Ta_2O_5−ZrO_2 samples.

CO has been widely used for probing Lewis acidity and to a lesser extent Brönsted acidity.[17,29] In the latter case, the weak interaction between CO and acidic hydroxyls leads to strong vibrational changes in OH stretching vibrations due to hydrogen bonding. It was shown that, for zeolitic materials, the ν(OH) shift caused by the interaction can be used as a measure of the acid strength of hydroxyls.[29] Figure 13 illustrates the spectral development in the CO and OH stretching regions for physically adsorbed CO on 9TaZr at 77 K as CO pressure is increased. It can be seen that there are at least two main different types of adsorbed CO species. The first type is characterized by a broad and complex band progressively shifting from 2179 to 2170 cm^{-1} and attributed to CO adsorbed on Zr^{4+}_{cus} sites at the surface of ZrO_2[30] left uncovered by Ta. Interestingly, this band was shown to decrease with a further increase in Ta loading, which is consistent with the increasing coverage of the ZrO_2 surface by Ta. The second type of adsorbed CO species is characterized by a band evolving at ca. 2154 cm^{-1} with increasing CO pressure and is attributed to CO H-bonded to polar hydroxyls still present at the surface of the catalyst. The development of the band at 2154 cm^{-1} is accompanied by the appearance of a broad OH band at ca. 3610 cm^{-1} and the decrease in the intensity of the ν(OH) bands at 3753 and 3680 cm^{-1}. To obtain from these experiments more quantitative data concerning Brönsted acidity, we must note two important points: (i) In all experiments, no further major spectral changes could be observed beyond 2.5 Torr CO pressure. As a consequence, spectra recorded at this pressure were considered as characteristic of full coverage of OH by CO. (ii) The contribution of ZrO_2 hydroxyls to CO adsorption became negligible when Ta loading was increased. The ν-(OH) shift of the band at ca. 3750 cm^{-1} caused by CO interaction at 2.5 Torr CO could therefore be considered in most cases as indicative of the acid strength of hydroxyls mainly bonded to Ta species. Figure 14 shows the variation of ν(OH) shift and ν(CO) of CO adsorbed on Ta−OH vs Ta content. Clearly, only minor variations are observed for the position of ν(CO) vibration with Ta content. This shows that ν(CO) is not very sensitive for measuring the strength of Brönsted acid sites. In contrast, the ν(OH) shift varies strongly with Ta content. Interestingly this variation is small for low Ta content and large for Ta_2O_5 exceeding 40% w/w. It may be inferred that much stronger Brönsted acidity is generated when a Ta_2O_5 phase is present at the surface of ZrO_2, i.e., for Ta_2O_5 content higher than 40% w/w.

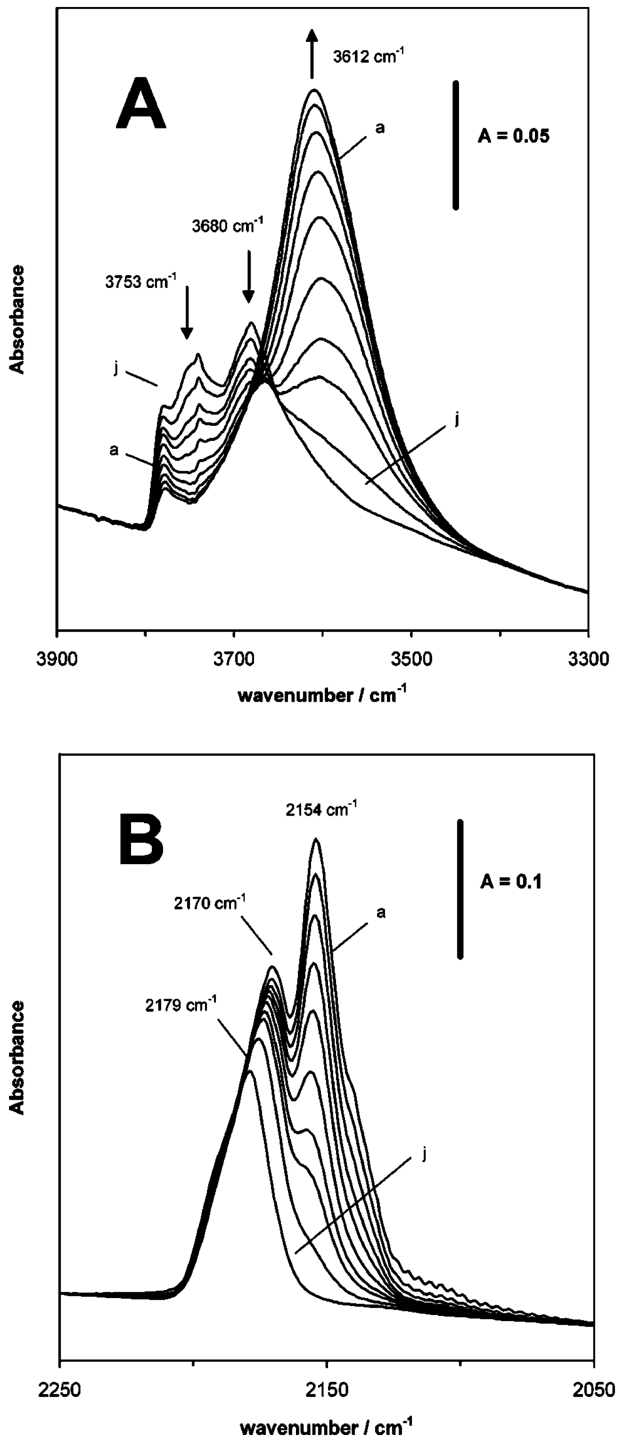

Figure 13. FTIR spectra of the 9TaZr sample after CO adsorption at 77 K. (A) ν(OH) region; (B) ν(CO) region. The CO pressure was successively adjusted to 10, 5, 2.5, 1.3, 0.7, 0.4, 0.2, 0.1, 0.05, and 0.02 Torr from spectrum a to spectrum j.

---

(28) Corma, A.; Rodellas, C.; Fornes, V. *J. Catal.* **1984**, *88*, 374.
(29) Garrone, E.; Chiappetta, R.; Spoto, G.; Uglienzo, P.; Zecchina, A.; Fajula, F. *Proceedings from the Ninth International Zeolite Conference*; von Ballmoos, R., Higgins, J. B., Treacey, M. M. J.; Butterworth-Heinemann: Boston, 1993, Vol II, p 267.
(30) Ferraris, G.; De Rossi, S.; Gazzoli, D.; Pettiti, I.; Valigi, M.; Magnacca, G.; Morterra, C. *Appl. Catal., A* **2003**, *240*, 119.

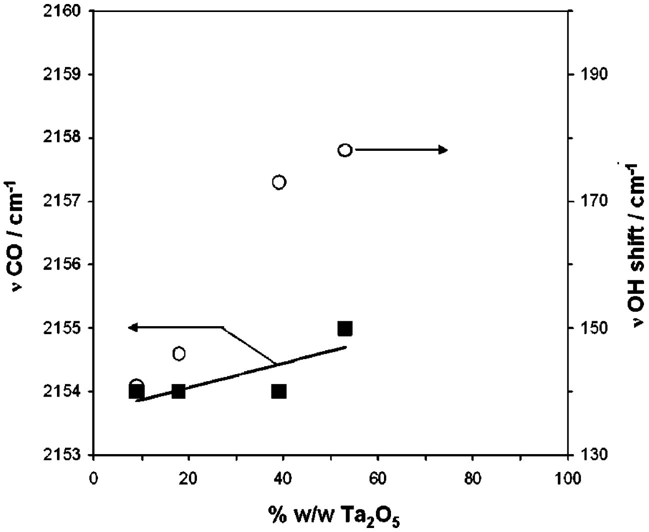

Figure 14. υ(CO) of CO adsorbed at 77 K ($P_{CO} = 2.5$ Torr) onto $Ta_2O_5-ZrO_2$ samples and the corresponding υ(OH) shift of the band at ca. 3750 cm^{-1}, caused by CO interaction as a function of Ta_2O_5 content.

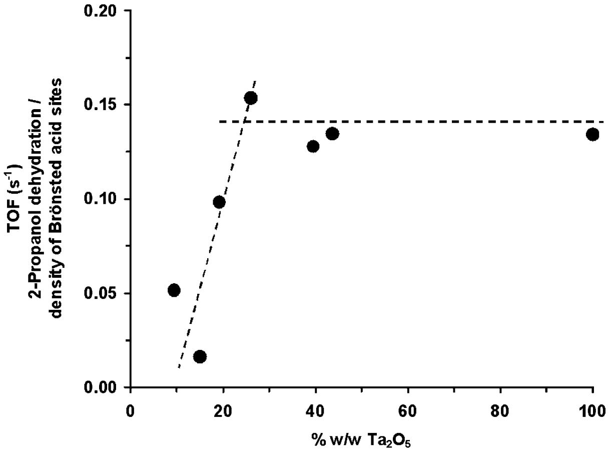

Figure 15. TOF of 2-propanol dehydration to propene referred to acid centers determined by lutidine adsorption vs Ta content. Acid centers determined after lutidine desorption at 523 K. Reaction conditions $T =$ 453 K, $P_{2-\text{propanol}} = 1.2$ kPa, GHSV $= 5400$ h^{-1}.

Devolopment of the Catalytic Activity with the Tantalum Content. For a better knowledge of the acidic surface properties of samples, we studied materials in the 2-propanol dehydration reaction, which was used to evaluate properties of several materials as acidic catalysts. The surface Brönsted acidity of several ZrO_2-based binary systems has been demonstrated to correlate with their catalytic behavior in 2-propanol dehydration reaction.[6,9]

Catalysts were tested in the reaction of 2-propanol at 453 K. In all cases, selectivities higher than 95% to propene were obtained, no acetone was detected, and only small amounts of diisopropyl ether were observed. The results of the propene formation rate are depicted in Figure 11 as a function of tantalum content. ZrO_2 and solids with low tantalum content show negligible activity in 2-propanol conversion. However, for a tantalum content higher than 15% w/w Ta_2O_5, a sharp increase in the activity is encountered up to samples with ca. 45% w/w Ta_2O_5.

Surface Structure/Acidity/Catalytic Activity Relationship. Figures 11 and 12 illustrate the correlation between the density of Brönsted acid sites determined after lutidine desorption at 523 K and the activity of samples in 2-propanol conversion. An increase in both parameters from a Ta_2O_5 content close to the monolayer value (ca. 15−20% w/w Ta_2O_5, 7−9 Ta atom/nm^2) to ca. 45% w/w Ta_2O_5 is encountered. We recall that CO adsorption experiments showed a relation between the Brönsted acidity and OH groups bonded to tantalum species (responsible for the IR band at ca. 3750 cm^{-1}). These experiments made it possible to determine that the strength of Brönsted acid centers increases with the increase in Ta content from 15 to 45% w/w Ta_2O_5. As stated above, an increase in tantalum content up to ca. 15−20% w/w Ta_2O_5 (monolayer value) produced the progressive coverage of ZrO_2 by surface tantalum species. For higher percent w/w Ta_2O_5 than 20% w/w, polymerized tantalum species and oxyhydrate tantalum aggregates formed. The presence of amorphous Ta_2O_5 aggregates in samples containing ca. 40% w/w Ta_2O_5 is related to the increased strength of Brönsted acid sites in these samples with respect to samples with lower Ta content.

Results plotted in Figures 11 and 12 indicate that the abundance of Brönsted acid sites determined by lutidine adsorption is directly related to the propene formation. The turnover frequency (TOF) values expressed as the propene formation activity per acid site[6] were calculated for the $Ta_2O_5-ZrO_2$ system. The results are represented in the Figure 15 as a function of the Ta_2O_5% w/w. The TOF values increased up to a Ta_2O_5 content of about 30% w/w and then remained almost constant up to pure Ta_2O_5 (see Figure 15). These facts suggest that surface Brönsted acid sites of Ta_2O_5 aggregates are responsible for the higher intrinsic activity shown by the samples with a Ta_2O_5% w/w content higher than 30%; these samples were shown by CO adsorption to have Brönsted acid sites of higher strength than samples with lower Ta_2O_5 content.

Acknowledgment. We thank MCYT (MAT2005-03456) and CIRIT 2005SGR-00184 for financial support.

CM062704Z